AVERAGE PHOTOSPHERIC POLOIDAL AND TOROIDAL MAGNETIC FIELD COMPONENTS NEAR SOLAR MINIMUM

THOMAS L. DUVALL, JR.*, PHILIP H. SCHERRER, LEIF SVALGAARD, and JOHN M. WILCOX

Institute for Plasma Research, Stanford University, Stanford, Calif. U.S.A.

(Received 1 July; in revised form 15 November, 1978)

Abstract. Average (over longitude and time) photospheric magnetic field components are derived from 3′ Stanford magnetograms made near the solar minimum of cycle 21. The average magnetograph signal is found to behave as the projection of a vector for measurements made across the disk. The poloidal field exhibits the familiar dipolar structure near the poles, with a measured signal in the line Fe I λ5250 Å of ≈1 G. At low latitudes the poloidal field has the polarity of the poles, but is of reduced magnitude (≈0.1 G). A net photospheric toroidal field with a broad latitudinal extent is found. The polarity of the toroidal field is opposite in the nothern and southern hemispheres and has the same sense as subsurface flux tubes giving rise to active regions of solar cycle 21.

These observations are used to discusse large-scale electric currents crossing the photosphere and angular momentum loss to the solar wind.

1. Introduction

Daily full-disk magnetograms made at Stanford with a spatial resolution of 3′ are used to study the average components of the large-scale solar magnetic field near the minimum of solar cycle 21. The daily magnetograms and measurements of the mean (integrated light) solar magnetic field (Scherrer *et al.*, 1977) are the main components of the long-term observing program at Stanford, which has the goal of observing the large-scale magnetic and velocity fields on a synoptic basis for at least one solar cycle. As part of the magnetogram observations, full-disk doppler line shifts are also observed. The result of the first year of velocity measurements will be discussed in a separate paper (Duvall, 1979).

2. Observations

The Stanford magnetograph has been discussed elsewhere (Scherrer *et al.*, 1977; Dittmer, 1977; Duvall, 1977). The light path for the 3′ magnetograms is shown in Figure 1. A 6.1 cm solar image is scanned boustrophedonically to make the magnetogram. A systematic error, normally less than 0.1 G, is measured both before and after the magnetogram by observing the magnetic signal on the nonmagnetic ($g = 0$) line Fe I λ5124 Å (Duvall, 1977b). This systematic error is subtracted from the magnetic measurements by making a linear interpolation between the two error signal measurements. The image is stepped ~1.5′ in the direction perpendicular to the solar rotation axis and ≈3′ in the other direction. The magnetic signal is

* Now at Kitt Peak National Observatory, Tucson, Ariz. 85726, U.S.A.

Solar Physics **61** (1979) 233–245. 0038–0938/79/0612–0233 $01.95.

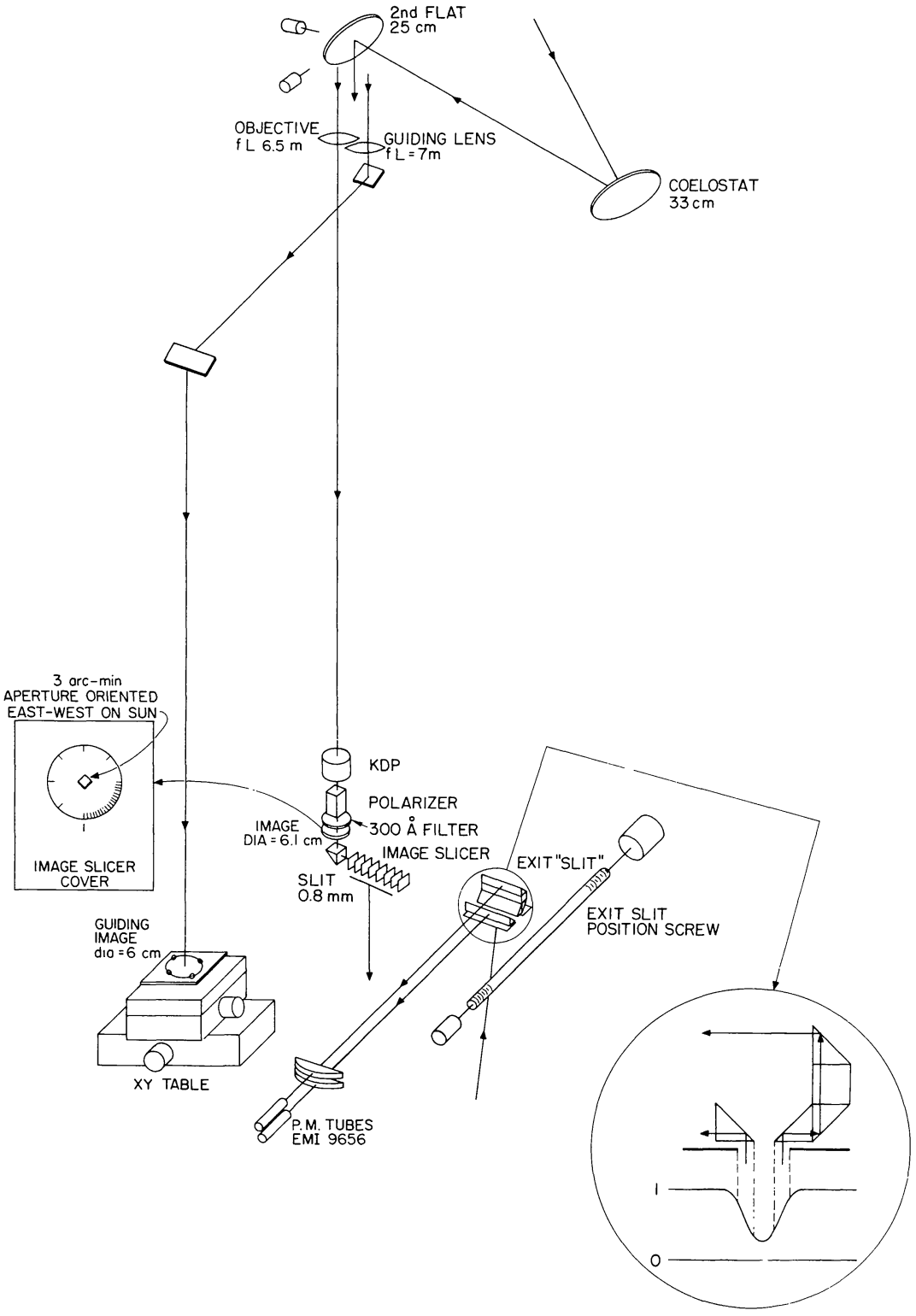

Fig. 1. Telescope light path. A two mirror coelostat system feeds the telescope. A 6.1 cm solar image is formed at the entrance slit to the spectrograph. The portion of this image which enters the spectrograph is controlled by the xy positioning table. The four photodiodes attached to the table control the position of the second flat mirror. The KDP and polarizer make up the modulated circular analyzer. The 300 Å filter suppresses overlapping orders from the grating. The image slicer converts the square entrance aperture into a slit 0.8 m × 100 mm. Upon return from the grating the light from the wings of an absorption line is

integrated at each position for 15 s. The statistical uncertainty of each measurement is ≈0.05 G. Two magnetograms observed on successive days are shown in Figure 2. The stability of the large-scale solar magnetic field from one day to the next is apparent. The observations used in the present study are 291 full-disk magnetograms covering May 1976–June 1977.

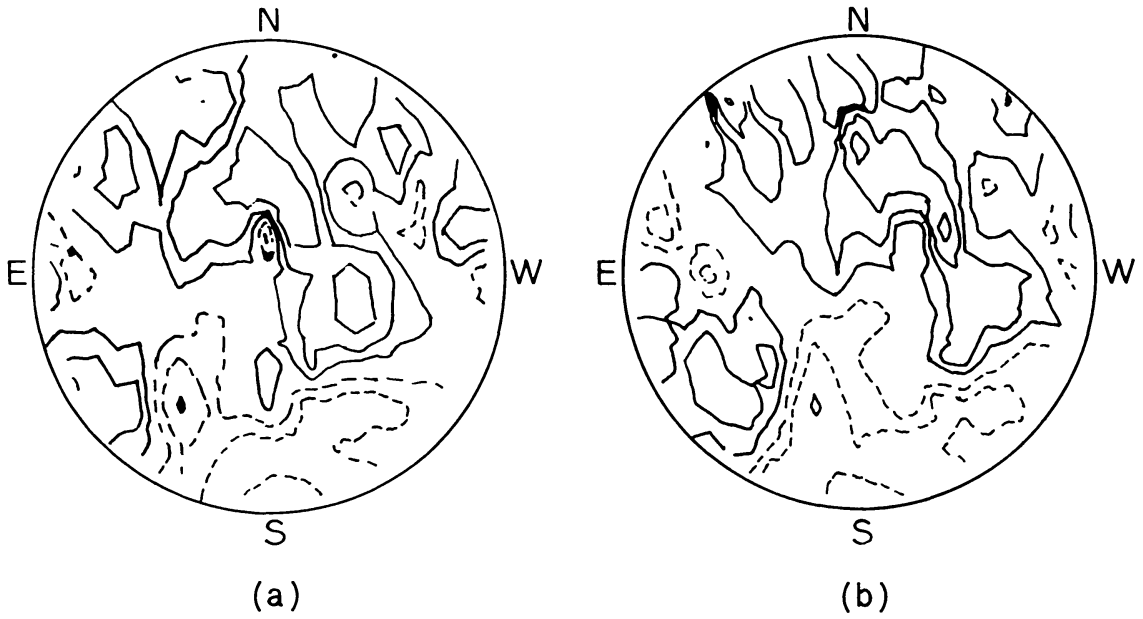

Fig. 2. Magnetograms made at Stanford with 3′ resolution (≈1/10 of the solar diameter). The spectral line used is Fe I λ5250.2 Å. The statistical error is approximately 0.05 G for each datapoint. The contour levels shown are ±0.2, ±0.5, ±1.0, ±2.0 G. (a) May 5, 1976. (b) May 6, 1976.

Suppose that a single region with constant magnetic field **B** is rotating across the solar disk. The region is shown at longitude ϕ with respect to central meridian in Figure 3. The component of **B** in the line of sight (B_l) of the observer at Earth as a function of ϕ is given by

$$B_l = B_\rho \cos\phi - B_\phi \sin\phi, \tag{1}$$

where B_ρ is the poloidal component of field in a cylindrical coordinate system defined with the z-axis being the solar rotation axis. (The inclination of the Sun's pole toward the Earth will be neglected in this analysis. Consideration of this tilt results in an average correction <1% to derived field components). By forming the time average

extracted by the prism and blind arrangement shown. The prism arrangement is mounted on ways that are positioned by a precisely machined screw. During observation, the exit slit assembly is maintained in the proper position by a servo system. Doppler shifts are observed by measuring the rotation of the screw. The spectrograph is not shown.

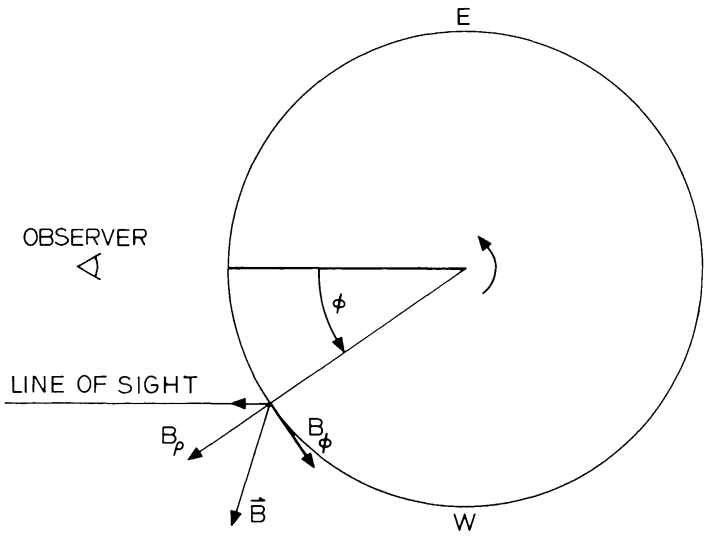

Fig. 3. Definitions of the different field components. The circle represents a latitude circle. The inclination of the solar rotation axis to the ecliptic is neglected. ϕ is the longitude measured with respect to the central meridian. B_ρ is the component of magnetic field projected into a plane parallel to the solar equator, positive outward. B_ϕ is the azimuthal field, measured positive in the direction of solar rotation. **B** is the resultant of B_ρ, B_ϕ. Also shown is **B** projected onto the observer's line of sight. This projection gives $B_l = B_\rho \cos\phi - B_\phi \sin\phi$.

at each value of ϕ by using many days' magnetograms, the average line of sight field is found:

$$\overline{B_l} = \overline{B_\rho} \cos\phi - \overline{B_\phi} \sin\phi \,. \tag{2}$$

Because the Sun rotates, the average components $\overline{B_\rho}$, $\overline{B_\phi}$ are both time and longitude averages.

This calculation is a simple model for how the average magnetograph signal might behave as a function of ϕ. This model will now be compared with observations. For each day's observation and for each measurement the average value of $\sin\phi$ and $\sin\lambda$ (λ = solar latitude) is calculated. To form the averages $\overline{B_l}(\sin\lambda, \sin\phi)$, each measurement is put into a bin depending on its value of $\sin\lambda$ and $\sin\phi$. The total range in $\sin\lambda$ (-1 to 1) is broken up into 11 parts as is the range in $\sin\phi$. $\sin\lambda$ and $\sin\phi$ are used instead of latitude and longitude because they are proportional to distance in the north–south and east–west directions. The averaged measured signal as a function of $\sin\phi$ for one of the latitude strips is shown in Figure 4. The signal at the center of the disk is nonzero, implying a nonzero radial component $\overline{B_\rho}$. The signals at the east and west limbs are not the same, implying a nonzero toroidal component $\overline{B_\phi}$. The curve plotted in Figure 4 is a least-squares fit to an expression of the form $\overline{B_l} = \overline{B_\rho} \cos\phi - \overline{B_\phi} \sin\phi$, where $\overline{B_\rho}$ and $\overline{B_\phi}$ are variable parameters.

To show that Equation (2) is the proper form to use in fitting the results, it is possible to fold the data across the central meridian in two different ways to obtain the components that are symmetric and antisymmetric with respect to the central meridian. Then we must show that the symmetric part is linear in $\cos\phi$ and the

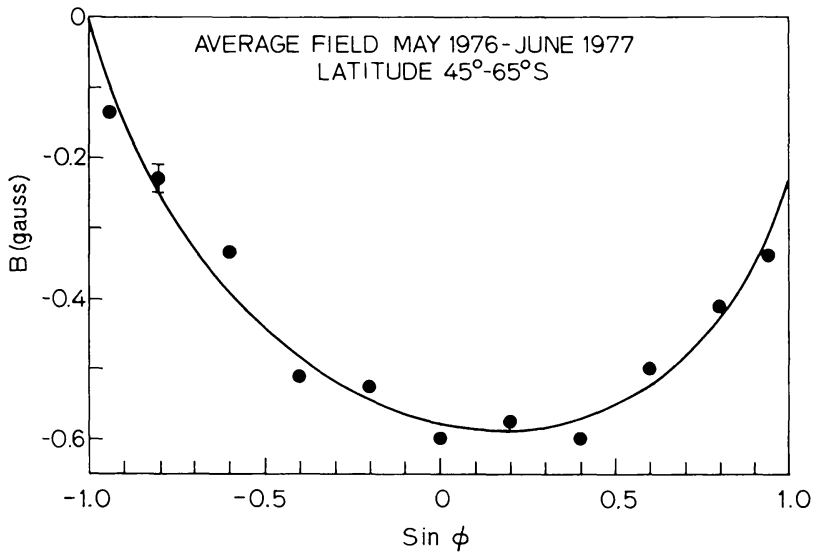

Fig. 4. Average field measured as a function of sin ϕ for a latitude strip 45°–65° S for May 1976–June 1977. sin ϕ corresponds to distance measured across the disk, with sin $\phi = -1$ for the east limb and sin $\phi = +1$ for the west limb. The error bar shown is twice the standard error of the mean. The curve is a least-squares fit to an expression of the form $B_l = B_\rho \cos\phi - B_\phi \sin\phi$.

antisymmetric part is linear in sin ϕ. The results of folding the data of Figure 4 are shown in Figure 5. In Figure 5(a) the antisymmetric component is derived, given by the expression

$$\overline{B_\phi} = \frac{\overline{B_l}(\phi) - \overline{B_l}(-\phi)}{2}. \tag{3}$$

In Figure 5(b) the symmetric component is derived, given by the expression

$$\overline{B_\rho} = \frac{\overline{B_l}(\phi) + \overline{B_l}(-\phi)}{2}. \tag{4}$$

The antisymmetric component is linear in sin ϕ and the symmetric component is linear in cos ϕ. From Figure 5 it is concluded that the average magnetograph signal behaves as the line of sight component of an average field vector for measurements made across the disk. This is in contrast to the claim of Howard and Stenflo (1972) that the magnetograph signal in the 5250 Å line falls off more slowly than cos ϕ. The source of the discrepancy is not understood. Values of $\overline{B_\rho}$, $\overline{B_\phi}$ were calculated for the 11 latitude belts. Uncertainties were estimated for $\overline{B_\rho}$, $\overline{B_\phi}$ by using the errors of the mean of each point going into the fit. For all values of $\overline{B_\rho}$, $\overline{B_\phi}$ the uncertainties were less than 0.01 G.

The poloidal field $\overline{B_\rho}$, derived by the fitting procedure described above, is shown as a function of latitude in Figure 6. The measured signal near the poles is found to be of magnitude ~1 G, positive in the north and negative in the south. The polarity of the poles extends to within 10° latitude of the equator in both hemispheres. The

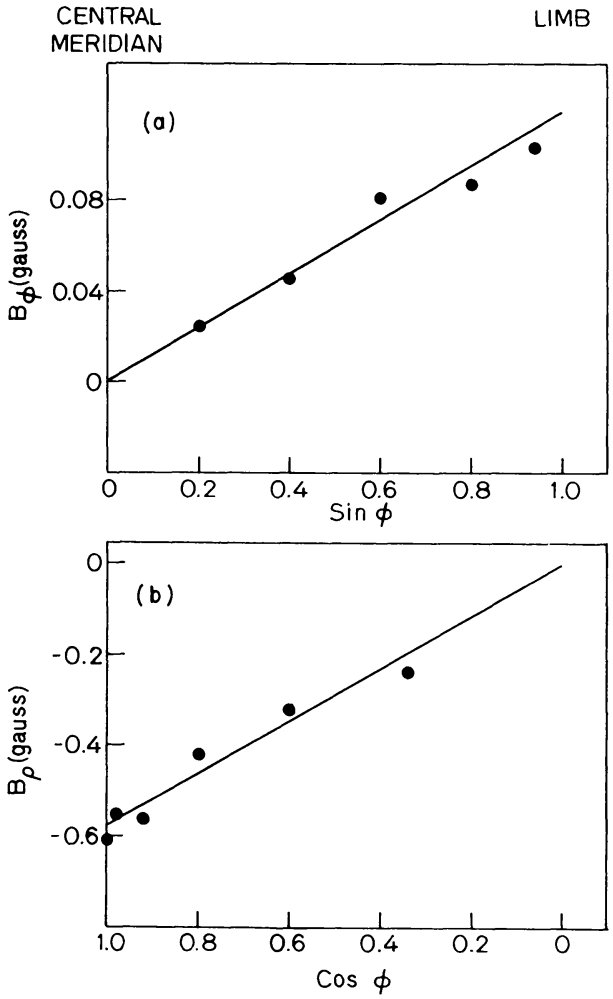

Fig. 5. (a) The antisymmetric component (about central meridian) of the average field signal plotted in Figure 4 as a function of sin ϕ. The line plotted corresponds to the azimuthal component derived from the fit $\overline{B_l} = \overline{B_\rho} \cos\phi - \overline{B_\phi} \sin\phi$ shown in Figure 4. (b) The component symmetric about central meridian as a function of cos ϕ. The line plotted is from the fit of Figure 4.

magnitude of the low-latitude poloidal field is small, on the order of 0.1 G. Its existence, however, may have large implications for models of the solar cycle.

The toroidal field $\overline{B_\phi}$, derived from the fitting procedure, is shown as a function of latitude in Figure 7. The sense of the toroidal field is opposite in the northern and southern hemispheres. The sense is the same as that of the assumed subsurface flux tubes giving rise to active regions in solar cycle 21. The toroidal field for the two halves of the observing period is shown in Figure 8. The field at latitudes 18°–30° in both hemispheres increased by a factor ~3 during this time period while at other latitudes the field remained approximately constant. There was more solar activity during the second half of the observing period and so the increase is attributed to the toroidal field of the active regions (or their remnants). No systematic time variation of the poloidal field was observed. The result that a mean azimuthal field is present is consistent with Howard's (1974) observation that field lines of the two polarities can be inclined toward each other or away from each other on the average.

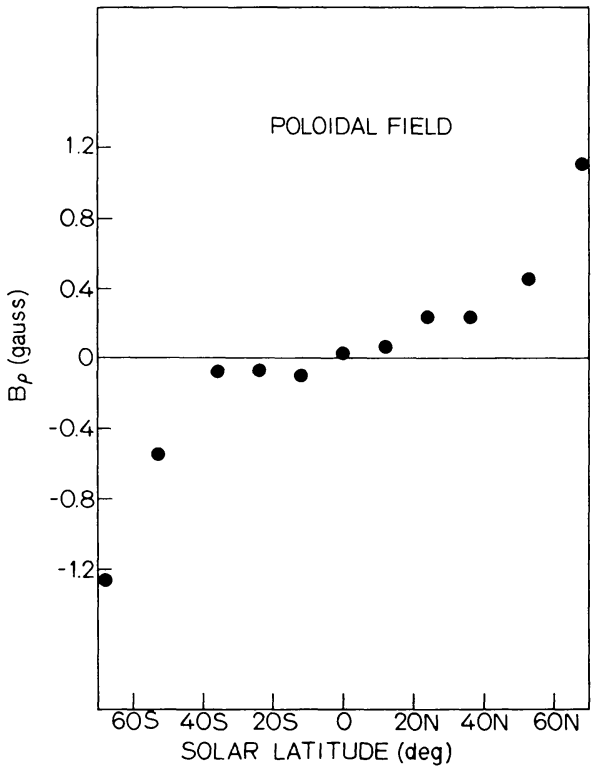

Fig. 6. Average poloidal field for May 1976–June 1977 as a function of solar latitude. Each point represents the results of a fit to the expression $\overline{B_l} = \overline{B_\rho} \cos \phi - \overline{B_\phi} \sin \phi$ for the latitude in question.

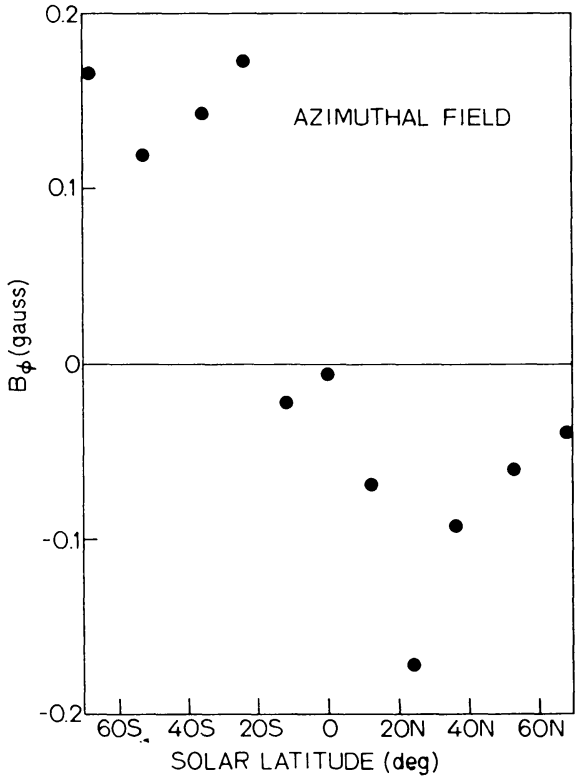

Fig. 7. Average toroidal field as a function of latitude for May 1976–June 1977. Each point represents a fit to the expression $\overline{B_l} = \overline{B_\rho} \cos \phi - \overline{B_\phi} \sin \phi$ for the latitude in question.

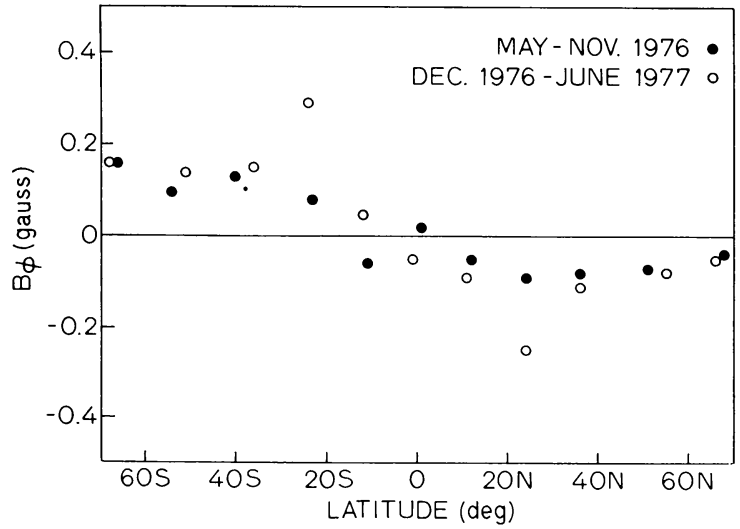

Fig. 8. The mean toroidal field as a function of latitude for the time periods May-Nov. 1976(●) and Dec. 1976–June 1977(○). The calculated errors are about the size of the dots.

3. Discussion

3. Electric current system

One consequence of the photospheric toroidal field is the existence of large-scale electric currents crossing the photosphere. Consider Ampére's law

$$\nabla \times \mathbf{B} = \frac{4\pi}{c}\mathbf{J}, \tag{5}$$

integrated over a surface defined by the portion of the spherical solar surface north of a certain latitude circle:

$$\int \nabla \times \mathbf{B} \cdot d\mathbf{S} = \frac{4\pi}{c} \int \mathbf{J} \cdot d\mathbf{S}. \tag{6}$$

The right side is $(4\pi/c)I$, where I is the current crossing the surface. The left side can be transformed, using Stoke's theorem, to a line integral along the latitude circle:

$$\oint \mathbf{B} \cdot d\mathbf{l} = \frac{4\pi}{c} I. \tag{7}$$

The average toroidal field is

$$\overline{B_\phi} = \frac{\oint \mathbf{B} \cdot d\mathbf{l}}{2\pi R_\odot \cos\lambda}. \tag{8}$$

We can write the total current crossing the photosphere at latitudes north of the one in question as

$$I = \frac{c}{2} R_\odot \cos\lambda \, \overline{B_\phi}. \tag{9}$$

To get all units in familiar terms, I will be expressed in ampère. The equation then becomes

$$I = 3.5 \times 10^{10} \overline{B_\phi} \cos \lambda \text{ (A)}, \tag{10}$$

where $\overline{B_\phi}$ is expressed in G. Taking $\lambda = 24°$ N, $\overline{B_\phi} = 0.172$ G, we find $I = -5.5 \times 10^{10}$ A, the negative sign implying that current is flowing into the Sun at latitudes greater than 24° N. A similar analysis shows that a similar magnitude current is flowing into the sun at southern latitudes greater than 24° S, leading to a total current in the circuit of 1.1×10^{11} A. By using different surfaces to integrate Ampère's law, it is possible to calculate the current density crossing the photosphere as a function of latitude. The results of such a calculation are shown in Figure 9. We see that poleward of 20° latitude in both hemispheres current is flowing into the Sun across the photosphere. This current is balanced by current leaving the Sun equatorwards of 20° latitude.

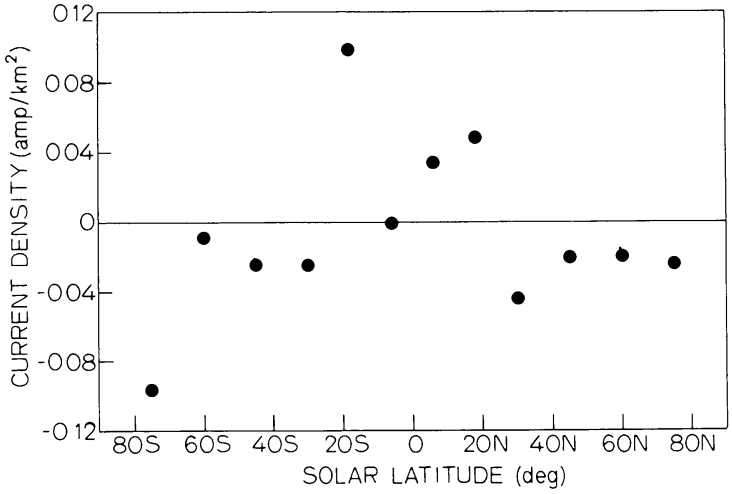

Fig. 9. Average current density crossing the solar photosphere as a function of latitude for the time period May 1976–June 1977. This current density is derived from the average toroidal field as described in the text. Positive current corresponds to current flowing out of the Sun.

Next, we will consider how far from the Sun does the current crossing the photosphere flow before returning. First, the current flowing in interplanetary space will be estimated using a simple model of the interplanetary magnetic field. The interplanetary field will be assumed to be of one polarity (positive) in the northern hemisphere and of the opposite polarity (negative) in the southern hemisphere. This model should be applicable near the solar minimum, when the interplanetary magnetic sectors are a small perturbation on the field (Schulz, 1973; Svalgaard and Wilcox, 1976; Alfvén, 1977). The Parker spiral model of the field will be assumed to be valid. The northern and southern hemispheres will be separated by a thin current sheet. Using the average azimuthal magnetic field measured at the Earth of 3×10^{-5} G, an outward current in this current sheet of 4.5×10^{9} A is calculated. This

current is balanced by an inward directed current of the same magnitude at higher latitudes in both hemispheres. We notice from Figure 8 that the currents crossing the photosphere are of the same sense: outwards near the equator and inwards at higher latitudes in both hemispheres. However, the radial interplanetary current is a factor ~25 smaller than the radial photospheric current. The results of this calculation are similar to those of Alfvén (1977). The magnitude of the radial interplanetary current is only 4% of the magnitude of the current crossing the photosphere and so it is concluded that the current crossing the photosphere does not flow throughout the heliosphere.

The radial component of the interplanetary current is a small fraction of the total large-scale interplanetary current. The azimuthal current in the current sheet separating the northern and southern hemispheres can be estimated by assuming a uniform field of positive polarity in the northern hemisphere, negative polarity in the southern hemisphere, and that the radial interplanetary field falls off as r^{-2}. A calculation using Ampère's law yields the total azimuthal current in the sheet as

$$I = -\frac{c}{2\pi} B_0 r_0^2 \left(-\frac{1}{r_h} + \frac{1}{R_0} \right) \tag{11}$$

(cgs units), where B_0 is the field strength at the reference distance r_0, r_h is the radius of the heliosphere, and R_0 is the inner boundary of the sheet. The term with r_h can be neglected. Assuming $R_0 = 2.6 R_\odot$, $B_0 = 3 \times 10^{-5}$ G, $r_0 = 1$ AU, this result reduces to $I = 0.6 \times 10^{11}$ A. 90% of this current flows between $2.6 R_\odot$ and $26 R_\odot$. The similarity in magnitude between this current and the current crossing the photosphere is suggestive of a physical connection.

3.2. Angular momentum flux

From solar wind plasma and interplanetary magnetic field observations, it has been estimated that the solar angular momentum loss rate (=torque on the Sun) is $\sim 10^{31}$ dyne-cm (Hundhausen, 1972). This torque is probably coupled to the Sun via the magnetic field, which tends to make the coronal plasma rotate with the photospheric angular rate. The magnetic field thereby deposits angular momentum in the coronal plasma. As the coronal plasma escapes to the solar wind it carries excess angular momentum, resulting in a torque on the Sun.

At the photospheric level the torque on the Sun will be exhibited as a magnetic stress. At a point on the photosphere the component about the rotation axis of the angular momentum flux is (Jackson, 1962)

$$M_z = -\frac{R_\odot}{4\pi} B_\rho B_\phi , \tag{12}$$

where B_ρ ($= B_r \sin\theta$) is the radial field in the cylindrical coordinate system and B_r is the radial component in a spherical polar coordinate system. The total torque is

derived by integrating this expression over the solar surface:

$$N = \int_s M_z \, da = -\frac{R_\odot}{4\pi} \int_s B_\rho B_\phi \, da = -R_\odot^3 \overline{B_\rho B_\phi}, \tag{13}$$

where now the mean value describes an average over the solar surface. If the solar fields were weak fields, and uncorrelated on a scale smaller than the aperture of the Stanford magnetograph, we would write $\overline{B_\rho B_\phi} = \overline{B_\rho}\,\overline{B_\phi}$. Under this assumption a calculation was made of the total torque using the calculated longitudinal averages $\overline{B_\rho}, \overline{B_\phi}$. The resulting value for the torque is 1.1×10^{31} dyne-cm, in remarkable agreement with the solar wind estimate.

The assumption $\overline{B_\rho B_\phi} = \overline{B_\rho}\,\overline{B_\phi}$ is, however, inconsistent with current ideas of solar magnetic fields as compressed into small bundles of field strength at least 10^3 G. Suppose that the observed mean fields were $\overline{B_\rho} = 1$ G, $\overline{B_\phi} = 0.1$ G. This would result in an estimate for $\overline{B_\rho B_\phi}$ of 0.1 G^2. If the field is made up of 10^3 G bundles covering $10^{-3}\, A_\odot$ ($A_\odot$ = solar surface area), a mean field $\overline{B_\rho}$ of 1 G would be observed. Tilting the flux tubes to yield $\overline{B_\phi} = 0.1$ G would require $B_\phi = 10^2$ G at the sight of the flux tube. The resulting value of $\overline{B_\rho B_\phi}$ is $10^3 \text{ G} \times 10^2 \text{ G} \times 10^{-3}\, A_\odot / A_\odot = 10^2$ G^2, a factor of 10^3 larger than the estimate using the product of mean values. Using this flux tube model with the present observations would then require that 1000 times as much angular momentum be crossing the photosphere as is observed in interplanetary space. There is independent evidence for this inconsistency with the flux tube model. By observing magnetic flux separately in the east and west hemispheres, Howard (1974) inferred that magnetic flux tubes are inclined trailing the rotation by a mean angle of 0°.8. Using this angle, his measured mean fields and the above flux tube model, the torque on the Sun was found to be a factor of 480 larger than the solar wind estimates.

Foukal (1977) suggests that Howard's 0°.8 tilt is due to the flux tubes being rooted in a deeper, more rapidly rotating layer. From the present considerations, this is seen to be inconsistent with angular momentum conservation.

One way to resolve the difficulty with the flux tube model would be to have the azimuthal field be a weak field. Then at the sites of the flux tubes (the only important places for calculating $\overline{B_\rho B_\phi}$ if the radial field is all in flux tubes) the toroidal field would be $\sim 10^{-1}$ G instead of 10^2 G, and the discrepancy would be resolved.

A simple model can be developed to explain the existence of the weak azimuthal field. It will be assumed that the torque of the solar wind is coupled to the Sun by the magnetic field. This coupling will be assumed to take place by large-scale currents generated in the high corona which flow along the magnetic field lines which connect to interplanetary space. It will be assumed that the flux tubes in the photosphere are radial. The large-scale current, which flows in the same sense, for example, over the region north of 40° latitude, will flow into the Sun along the flux tubes. The local effect of the current flowing along a single flux tube will be to make the field lines helical but will not make a net toroidal field. However, the long-range effect of all the currents flowing in the same sense north of 40° latitude will be a weak toroidal field (a

necessary consequence of Ampère's law). This type of a model should be applicable near solar minimum, when the interplanetary magnetic field has the symmetry of a north-south dipole and most of the interplanetary field comes from high-latitude solar fields. Near solar maximum, when the photospheric and interplanetary fields lose their north-south dipole-type symmetry, the geometry becomes more complicated but the main result must still hold: the intense flux tubes in the photosphere cannot be inclined trailing the rotation by an average of 0°.8 because too much angular momentum would be lost. The azimuthal field due to the torque of the solar wind must then be a weak field, which, near solar maximum, will not be axisymmetric.

4. Summary

The average poloidal and toroidal components of the photospheric magnetic field have been observed near the minimum of solar cycle 21. The direct observational results are:

(1) The poloidal field near this solar minimum has opposite polarities in the north and south hemispheres. The measured strength at high latitudes is ~1 G. The strength of the poloidal field falls off sharply towards low latitudes (much faster than a dipole) but has a measurable strength at low latitudes of ~0.1 G.

(2) A mean toroidal field of broad latitudinal extent is found. The toroidal field is of opposite sense in the northern and southern hemispheres and has a strength on the order of 0.1 G. The toroidal field in the latitudes 18°–30° was found to increase in strength by a factor ~3 during the 14 months of observations.

Several interpretations of these results and those of Howard (1974) have been made:

(1) The mean toroidal field implies the existence of large-scale electric currents crossing the photosphere. Current is flowing into the sun at all latitudes greater than 20°. The current is balanced by an outward current equatorwards of 20°. The total current flowing is 1.1×10^{11} A. Dividing this current by the solar surface area yields a typical current density of 0.02 A km^{-2}.

(2) The Maxwell stresses associated with the mean poloidal and toroidal magnetic fields yield a torque on the Sun which is comparable to that derived from solar wind observations. It is concluded that this torque is that due to the solar wind and that it is possible to observe this torque through observations of the photospheric field, which is the agent that couples the torque to the sun. It is concluded that the mean toroidal field has two sources: (i) the solar wind and (ii) a portion in the active latitudes associated with active regions as evidenced by the increase in the toroidal field in these latitudes as solar activity increases.

(3) It is shown that Howard's (1974) observation of a flux difference between the east and west solar hemispheres cannot be the result of flux tubes being inclined 0°.8 trailing the rotation, as this leads to too much angular momentum loss through the photosphere. This flux difference must be the result of weak azimuthal fields which are presumably generated by the torque of the solar wind.

Acknowledgements

We would like to thank Robert Howard and John Harvey for making helpful suggestions on a draft of this paper. This work was supported in part by the Office of Naval Research under Contract N00014-76-C-0207, by the National Aeronautics and Space Administration under Grant NGR 05-020-559, by the Atmospheric Sciences Section of the National Science Foundation under Grant ATM-20580 and the Max C. Fleischmann foundation.

References

Alfvén, H.: 1977, *Rev. Geophys. Space Phys.* **15**, 271.
Dittmer, P. H.: 1977, Ph.D. Thesis, Stanford University, Dept. of Applied Physics.
Duvall, T. L., Jr.: 1977, Ph.D. Thesis, Stanford University, Dept. of Applied Physics.
Duvall, T. L., Jr.: 1979, submitted to *Solar Phys.*
Foukal, P.: 1977, *Astrophys. J.* **218**, 539.
Howard, R.: 1974, *Solar Phys.* **39**, 275.
Howard, R. and Stenflo, J. O.: 1972, *Solar Phys.* **22**, 402.
Hundhäusen, A. J.: 1972, in C. P. Sonett, P. J. Coleman, Jr., and J. M. Wilcox (eds.), *Solar Wind*, Scientific and Technical Information Office, NASA, Washington, D.C., pp. 261–266.
Jackson, J. D.: 1962, *Classical Electrodynamics*, John Wiley and Sons, Inc., New York, p. 200.
Schatten, K. H.: 1973, *Solar Phys.* **32**, 315.
Scherrer, P. H., Wilcox, J. M., Svalgaard, L., Duvall, T. L., Jr., Dittmer, P. H., and Gustafson, E. K.: 1977, *Solar Phys.* **54**, 353.
Schulz, M.: 1973, *Astrophys. Space Sci.* **24**, 371.
Svalgaard, L. and Wilcox, J. M.: 1976, *Nature* **262**, 766.